

ResKACNNNet: A Residual ChebyKAN Network for Inertial Odometry

Shanshan Zhang, Tianshui Wen, Siyue Wang, Qi Zhang, Ziheng Zhou, Huiru Zheng, Lingxiang Zheng, Yu Yang

Abstract—Inertial Measurement Unit has become a focal point for achieving low-cost, precise positioning. However, conventional inertial positioning methods based on CNNs are limited in capturing nonlinear motion characteristics and long-term dependencies in IMU data. To address this issue, we propose a novel inertial positioning network with a generic backbone, ResChebyKAN, which leverages the nonlinear approximation capability of Chebyshev polynomials to model complex motion characteristics. Additionally, we introduce an Efficient Kernel-based Self-Attention module that effectively captures contextual information and enhances long-term dependency modeling. Experimental results on public datasets (e.g., RIDL, RoNIN, RNIN-VIO, OxiOD, IMUNet and TLIO) show that our approach reduces absolute trajectory error by 3.79% to 42.32% compared to existing benchmark methods. Furthermore, we release a pre-processed dataset and empirically demonstrate that removing the gravity component from acceleration data significantly improves inertial positioning performance.

Code Repository: Double Anonymous Review Process.

Index Terms—Inertial Positioning Network, Long-term learning, Localization

I. INTRODUCTION

INERTIAL Measurement Unit (IMU) typically consists of an accelerometer and a gyroscope, providing reliable three-axis acceleration and angular velocity data. Due to their independence from external environmental cues, low cost, and high update frequency, IMUs are widely applied in autonomous driving and indoor localization [1], [2]. In scenarios where external devices such as cameras, radars, or GPS are limited or unavailable, inertial positioning systems offer a crucial supplementary or alternative solution for positioning and navigation.

Conventional inertial positioning systems primarily rely on Newtonian mechanics for position computation. For example, the Strapdown Inertial Navigation System (SINS) [3] estimates positions by integrating and filtering IMU data; Pedestrian Dead Reckoning (PDR) [4] determines a user's position based on step detection, step length estimation, and heading calculation; and Zero Velocity Update (ZUPT) [5] mitigates positioning errors by exploiting the physical constraint of zero velocity during stationary intervals. However, these methods generally suffer from cumulative integration errors and are highly sensitive to motion states and sensor installation configurations, making them less suitable for complex application scenarios (e.g., in the wild [6]).

In recent years, data-driven inertial positioning methods have demonstrated the ability to extract more accurate positional information from IMU data while adapting to diverse motion patterns. For instance, RoNIN [6] infers velocity from IMU data by employing ResNet [7], TCN [8], and LSTM [9]

networks to estimate position; TLIO [10] combines a ResNet architecture with a Stochastic Cloning Extended Kalman Filter (SCEKF) [11] to further improve trajectory estimation accuracy; RNIN-VIO [12] leverages LSTM to enhance ResNet's sequential modeling capability, incorporating it as part of a Visual-Inertial Odometry (VIO) [13] system; IMUNet [14] constructs a network suitable for mobile devices using Depth-wise Separable Convolutions (DSC) [15] and compares its performance with lightweight networks such as MobileNet [16], MnasNet [17], and EfficientB0 [18]; SSHNN [19] fuses CNNs, convolutional attention mechanisms, and LSTM to build a hybrid inertial inference framework.

However, existing CNN and LSTM based inertial positioning methods still exhibit several limitations: (1) constrained feature learning capacity, hindering accurate capture of nonlinear motion characteristics; (2) insufficient modeling of long-term dependencies in IMU data; and (3) limited exploration of gravity's influence on inertial positioning performance.

To address these issues, this paper proposes a novel inertial positioning network architecture to achieve more precise inertial positioning. The main contributions of this work are summarized as follows:

- 1) We propose a novel Residual ChebyKAN backbone (ResChebyKAN) to enhance the learning of nonlinear motion characteristics.
- 2) We develop an Efficient Kernel-based Self-Attention (EKSA) module to improve the modeling of long-term dependencies in IMU data.
- 3) We investigate the impact of gravity on positioning accuracy and a gravity-compensated dataset along with the corresponding code.
- 4) We validate our approach through extensive experiments on multiple benchmark datasets, demonstrating its superiority over existing methods and the effectiveness of the proposed modules.

II. RELATED WORK

A. Inertial Positioning Methods

Positioning solutions based on Newtonian mechanics offer ultra-low-cost localization. SINS [3] transforms raw acceleration data into a unified navigation frame, removes gravitational components, and calibrates the measurements, displacement is then obtained through double integration. However, this approach relies on high-precision IMU devices, typically used in aircraft or vehicle localization. Additionally, during the integration process, errors accumulate continuously, making long-distance positioning unreliable. PDR mitigates this issue by incorporating prior knowledge of human motion,

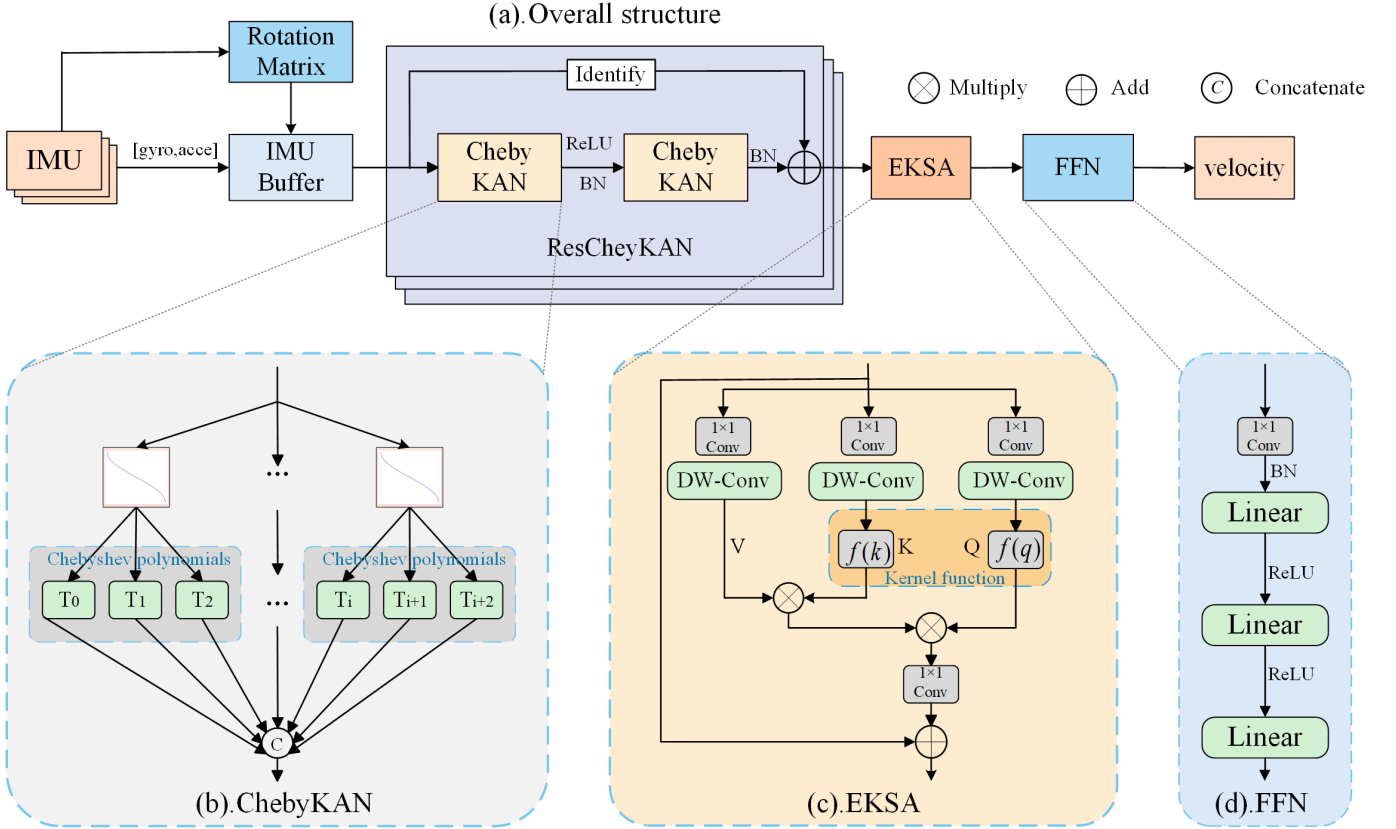


Fig. 1. The Overall Architecture of the Proposed Residual ChebyKAN Network for Inertial Positioning (ResKACNNNet), which primarily consists of ResCheyKAN incorporating ChebyKAN units and an Efficient Kernel-based Self-Attention (EKSA) mechanism.

including steps detection, stride length estimation, and heading information for positioning. A computationally simpler approach, Step Counting (SC) [20], estimates displacement as the product of step length and step count, where step length is either constant or dynamically estimated. However, this method struggles to adapt to diverse motion scenarios, such as outdoor environment, limiting its overall reliability.

Data-driven positioning solutions have further improved localization accuracy. IONet [21] proposed a bidirectional LSTM architecture that leverages dynamic context and outputs polar vectors to predict displacement information. RIDI [22] utilizes Support Vector Machine(SVM) [23] to classify device placements and estimates two-dimensional velocity using separate SVM models. RoNIN [6] introduced ResNet, LSTM, and TCN to estimate two-dimensional velocity, integrating them to obtain displacement information, which laid the foundation for subsequent research. TLIO [10] directly predicts displacement and its associated uncertainty using ResNet, and refine the displacement through SCEKF. Similarly, RNIN-VIO [12] integrates displacement and uncertainty predictions into a VIO system, introducing a combined loss function for displacement and velocity estimation.

IDOL [24] first employs a recurrent neural network and an EKF to obtain orientation estimates, transforming raw IMU measurements into an appropriate reference frame. It then utilizes another recurrent network architecture is used to obtain localization information. RIO [25] leverages rotational

equivariance as a self-supervisory signal, reducing dependence on large labeled datasets and enabling model adaptation to diverse unlabeled data. CTIN [26] applies Transformers to inertial positioning, incorporating local and global attention mechanisms to capture contextual information within motion trajectories. iMOT [27] proposes a novel inertial transformer encoder-decoder network that exploits the complementary effects of motion and rotation patterns for enhanced uncertainty modeling.

B. Dataset

Datasets are a cornerstone for research in data-driven inertial positioning. While most inertial positioning studies have made significant progress using gravity-compensated datasets, a systematic investigation into the necessity of gravity removal remains lacking. To bridge this gap, this paper applies gravity removal to the TLIO dataset (hereafter referred to as TLIOv2) and conducts comparative experiments to validate its crucial role in improving inertial positioning accuracy.

III. METHOD

In this section, we first present the overall pipeline of the proposed ResKACNNNet model. We then provide a detailed explanation of its implementation, including the ResCheyKAN backbone and the Efficient Kernel-based Self-Attention (EKSA) module. The impact of gravity is analyzed separately in the experimental section.

TABLE I
DESCRIPTION OF PUBLIC DATASETS USED FOR EVALUATION OF INERTIAL POSITIONING MODELS.

| Dataset | Ground Truth | Duration(hours) | Gravity Removed |
|----------|-----------------------|-----------------|-----------------|
| RIDI | Google Tango phone | 1.6 | Yes |
| IMUNet | ARCore | 9.0 | Yes |
| RNIN-VIO | Motion Capture System | 27.0 | Yes |
| RoNIN | Asus Zenfone AR | 42.7 | Yes |
| TLIO | VIO | 60.0 | No |
| TLIOv2 | VIO | 60.0 | Yes |

A. Overall Pipeline

The overall structure is illustrated in Fig. 1(a). Given the raw IMU measurement data $\mathbf{x} \in \mathbb{R}^{C \times 1}$, where $C = 6$ represents the input data dimensions (comprising acceleration and angular velocity), the data is first rotated into a unified localization coordinate system. It is then buffered to form an input window of size W , resulting in $\mathbf{X} \in \mathbb{R}^{C \times W}$, where W corresponds to the sensor's sampling rate.

In the backbone network, complex motion features are extracted through four stages, each consisting of two ResChebyKAN layers with specific feature dimensions and sequence lengths. At the end of each stage, the output dimensions of ResChebyKAN are adjusted to ensure compatibility across modules. ResChebyKAN adopts a classic residual structure composed of two fundamental ChebyKAN units. This design enables effective feature extraction with a relatively shallow network, ensuring stable training. Leveraging the superior nonlinear approximation capability of Chebyshev polynomials, ChebyKAN effectively captures the intricate motion features in IMU data. The feature learning process for the input data \mathbf{X} , can be calculated as:

$$\mathbf{X}_{\text{res}} = \text{ResChebyKAN}(\mathbf{X}) \in \mathbb{R}^{N \times L} \quad (1)$$

where N and L represent the extracted feature dimensions and sequence length, respectively.

To further enhance long-term dependency modeling, we introduce a kernel-based attention mechanism, EKSA module. Unlike conventional attention mechanisms that rely on computationally expensive attention matrices, EKSA replaces these operations with kernel functions, significantly, reducing computational complexity to linear.

Finally, the output of the EKSA module is mapped to a two-dimensional velocity representation through three fully connected layers and the model is optimized using the Mean Squared Error (MSE) loss function to ensure accurate velocity predictions.

B. Residual ChebyKAN

The convolutional layer is a crucial component of CNNs. However, traditional convolutions rely on fixed activation functions and linear transformations, limiting their ability to effectively capture complex features. Inspired by Kolmogorov-Arnold Network (KAN) [28], [29], researchers have replaced conventional fixed activation functions with learnable ones, enabling KAN-based convolutions to better capture rich features in images [30]–[32]. In this study, we propose and construct Residual ChebyKAN (ResChebyKAN) to enhance the network's capacity for extracting complex motion features.

Specifically, given input data or features $\mathbf{X} \in \mathbb{R}^{C \times W}$, we first partition the input into multiple groups based on a predefined number. For each grouped data x_i , a mapping is applied using the tanh and arccos functions as:

$$x' = \arccos(\tanh(x_i)) \quad (2)$$

Only values satisfying $\tanh(x_i) \in [-1, 1]$ are retained.

Next, we construct Chebyshev polynomials to extract complex features, forming a polynomial feature vector with a preset order d :

$$\mathbf{x}_{\text{poly}} = [T_0(x'), T_1(x'), \dots, T_d(x')] \quad (3)$$

where $T_n(x')$ denotes the Chebyshev polynomial of order n , which enhances the model's feature representation capability. Subsequently, \mathbf{x}_{poly} is mapped back to the original space via a cosine transformation and further encoded using a convolutional layer followed by normalization, yielding the output for that group. Finally, the outputs from all groups are then concatenated to form $\mathbf{X}_{\text{ChebyKAN}} \in \mathbb{R}^{C_{\text{ChebyKAN}} \times L_{\text{ChebyKAN}}}$.

By stacking ChebyKAN-based residual blocks, we construct a residual network backbone, refer to as ResChebyKAN, with the final output denoted as \mathbf{X}_{res} . By leveraging the superior function approximation capability of Chebyshev polynomials, ResChebyKAN effectively captures rich nonlinear motion characteristics, thereby enhancing its effectiveness in complex motion modeling.

C. Efficient Kernel-based Self-Attention (EKSA)

Attention mechanisms are widely employed to capture contextual information in both images and sequential data [33]. We first provide a brief overview of the self-attention mechanism. Given an input feature $\mathbf{X}_{\text{image}}$, it is projected through convolutional or linear transformations into query (Q), key (K), and value (V). The self-attention mechanism computes the dot product between all queries and keys, applies Softmax normalization, and then multiplies the result with the values to obtain the attention output. For single-head self-attention, this process can be formulated as:

$$\text{Self-Attention} = \text{softmax} \left(\frac{QK^\top}{\sqrt{\gamma}} \right) V \quad (4)$$

where γ is a predefined scaling factor. This mechanism effectively captures long-term dependencies in the data. However, its computational complexity is $\mathcal{O}(LN^2)$, posing a significant burden, especially for long sequences. To address this, various lightweight attention mechanisms have been proposed [34]. In this study, we introduce an efficient Kernel-based self-attention

TABLE II

OVERALL TRAJECTORY PREDICTION ACCURACY. THE BEST RESULT IS HIGHLIGHTED IN BOLD. WE CONDUCTED A COMPARATIVE EXPERIMENT ON GRAVITY REMOVAL IN BOTH TLIO AND TLIOv2. THE \downarrow INDICATES A DECREASE IN ERROR, WHILE THE \uparrow SIGNIFIES AN INCREASE.

| Dataset | Metric | RoNIN-ResNet | RoNIN-LSTM | RoNIN-TCN | SRNIN | IMUNet | STLIO | ResKACNNet | ResKACNNet Improvement over RoNIN-ResNet(%) |
|----------|--------|----------------------|------------|-----------|--------|--------------|--------|--------------|---|
| | | Performance (meters) | | | | | | | |
| RoNIN | ATE | 5.365 | 6.362 | 7.983 | 6.987 | 14.591 | 6.481 | 3.814 | 28.91 |
| | RTE | 3.390 | 3.518 | 3.647 | 3.438 | 7.967 | 3.746 | 3.272 | 3.48 |
| RIDI | ATE | 2.578 | 2.942 | 7.936 | 2.170 | 2.909 | 2.332 | 1.835 | 28.82 |
| | RTE | 2.823 | 3.405 | 7.971 | 2.296 | 3.335 | 2.524 | 1.954 | 30.78 |
| RNIN-VIO | ATE | 1.850 | 2.398 | 1.803 | 1.432 | 2.005 | 1.553 | 1.067 | 42.32 |
| | RTE | 2.185 | 3.150 | 2.199 | 1.776 | 2.631 | 1.865 | 1.260 | 42.33 |
| IMUNet | ATE | 14.207 | 9.841 | 44.184 | 15.174 | 11.847 | 19.958 | 9.023 | 36.49 |
| | RTE | 7.946 | 7.417 | 19.019 | 8.164 | 7.792 | 10.123 | 7.082 | 10.87 |
| TLIO | ATE | 1.476 | 2.451 | 3.254 | 1.572 | 1.432 | 1.493 | 1.420 | 3.79 |
| | RTE | 3.790 | 6.710 | 9.731 | 4.183 | 3.474 | 3.628 | 3.509 | 7.41 |
| TLIOv2 | ATE | 1.328↓ | 2.273↓ | 3.939↑ | 1.371↓ | 1.421↓ | 1.645↑ | 1.322↓ | - |
| | RTE | 1.105↓ | 1.684↓ | 2.215↓ | 1.122↓ | 1.116↓ | 1.227↓ | 1.118↓ | - |

strategy, EKSA, which models long-term dependencies in IMU data while maintaining linear computational complexity.

Given an input feature \mathbf{X}_{Res} , we first applies a 1×1 convolution followed by a depthwise convolution to project the input into query (Q), key (K), and value (V), all belonging to $\mathbb{R}^{N \times L}$. To reduce computational complexity and avoid direct inner product calculations between Q and K , we replace the inner product with the correlation coefficient, computed as:

$$\rho(q, k)^2 = \left(\frac{(q - E(q))(k - E(k))^\top}{\|q - E(q)\| \cdot \|k - E(k)\|} \right)^2 \quad (5)$$

where $E(q)$ and $E(k)$ denote the mean values of q and k , respectively. This measure remains invariant to scaling and translation, which improves robustness against common noise, including scaling and offset.

Next, we construct a Mercer kernel function using the kernel trick $\exp(\rho(q, k)^2)$. According to Mercer's theorem, this ensures the existence of a mapping function $f(\cdot)$ such that:

$$\exp(\rho(q, k)^2) = \langle f(q), f(k) \rangle \quad (6)$$

By applying a Taylor expansion to the kernel function, we derive an explicit expression for $f(q)$:

$$f(q) = \left(1, \frac{(q - E(q))^2}{\sigma^{\frac{1}{2}}}, \frac{(q - E(q))^4}{2^{\frac{1}{2}} \sigma}, \dots \right) \quad (7)$$

where σ is a hyperparameter that regulates the contribution of higher-order terms and the smoothness of the kernel function. As a result, the attention computation simplifies to:

$$\text{EKSA} = f(q)f(k)^\top V = f(q)(f(k)^\top V) \quad (8)$$

This reformulation significantly reduces the computational complexity from $\mathcal{O}(LN^2)$ to $\mathcal{O}(NL^2)$. Since, the feature dimension N generally grows much larger than the sequence length L as the network depth increases, this optimization leads to substantial efficiency gains.

IV. EXPERIMENTS

We conducted a series of comparative experiments using five publicly available datasets to evaluate the performance of

our proposed ResKACNNet, benchmarking it against widely recognized data-driven positioning methods. Additionally, we assessed the impact of gravity removal on positioning accuracy using the TLIO dataset. All models were retrained and evaluated on an NVIDIA RTX A40 GPU (48 GB).

A. Datasets

Table I summarizes the datasets used in our experiments. For all datasets, except for the TLIO dataset, the gravity component was removed during preprocessing, as reported in the original papers. Each dataset was partitioned into training, validation, and testing sets using an 8:1:1 split.

B. Comparison Methods

Unlike traditional Newtonian mechanics-based inertial positioning, data-driven approaches can directly infer more precise positioning information more accurately from IMU measurements [2]. This study focuses on the contribution of these data-driven methods to enhance inertial positioning accuracy. (i) RoNIN estimates position by inferring velocity from IMU data using ResNet, TCN, and LSTM networks. We utilized the open-source implementation provided in the original study for RoNIN. (ii) RNIN-VIO and TLIO integrate neural network-inferred displacements with VIO and SCEKF, respectively. However, since these hybrid approaches are not compatible with all public datasets, we retained only their neural network components, referring to them as SRNIN and STLIO in this study. (iii) IMUNet is a lightweight inertial positioning network for mobile devices using DSC. We used the open-source code provided in the original paper.

C. Evaluation Metrics

The model estimates positioning information by integrating the predicted velocities over time. To comprehensively assess its performance in inertial positioning tasks, we adopted the following metrics, as introduced in [35] and [26]:

- **Absolute Trajectory Error (ATE):** The ATE is defined as the root mean square error (RMSE) between the predicted and ground-truth trajectories. This metric reflects

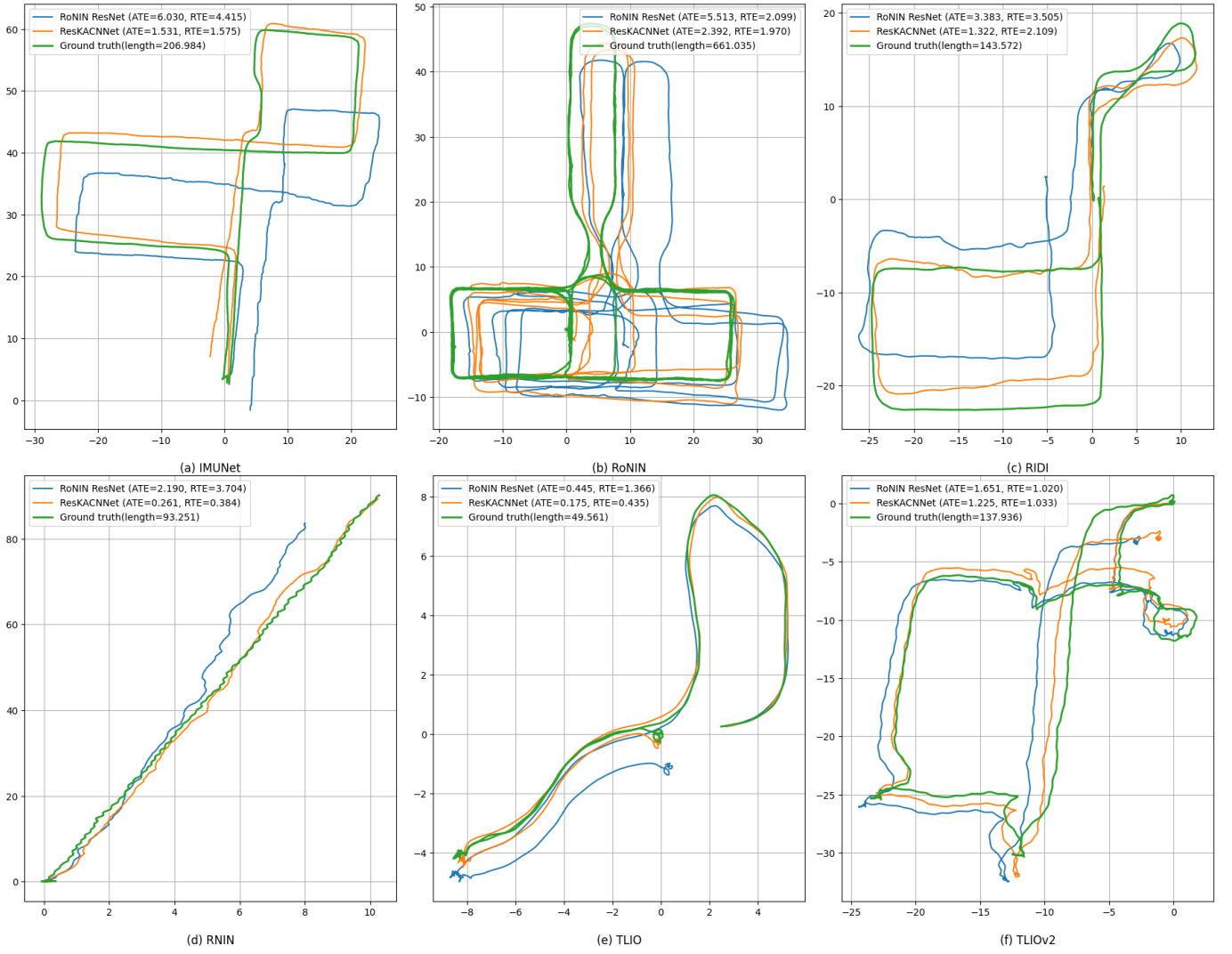


Fig. 2. Test data sample trajectories from the IMUNet, RoNIN, RIDI, RNIN-VIO, TLIO, and TLIOv2 datasets, along with the performance of all current state-of-the-art networks. The units of the X-axis and Y-axis are meters. The numbers in parentheses indicate the ATE and RTE errors (in meters) and the total length of the test trajectory (in meters). All axes are measured in meters. Subscripts indicate the dataset to which each trajectory belongs.

the overall quality of trajectory reconstruction, with lower values indicating greater positioning accuracy.

- **Relative Trajectory Error (RTE):** The RTE is computed as the RMSE between the predicted and ground-truth trajectories over a fixed time interval (which was set to 60 s in our experiments). It measures the accuracy of local trajectory reconstruction, with lower values indicating higher accuracy.
- **Position Drift Error (PDE):** The PDE quantifies the drift of the predicted final position relative to the entire trajectory, providing further insight into the model's precision. Its value is inversely proportional to positioning accuracy.

D. Result Analysis

Table II presents the experimental results for all models across five public datasets. The findings demonstrate that ResKACNNet consistently outperforms other models on most datasets, achieving significantly lower ATE and RTE values, except for the TLIO dataset, where its performance is slightly

less accurate. In inference experiments conducted on the TLIO dataset, IMUNet yields a lower RTE than ResKACNNet. Specifically, compared to the classical RoNIN-ResNet model, ResKACNNet achieves a reduction in ATE of 3.79%–42.32% and a reduction in RTE of 3.48%–42.33% across all test datasets.

The primary limitations of RoNIN-ResNet, SRNIN, and STLIO stem from their dependence on conventional convolutions for feature extraction, which struggle to fully capture the nonlinear motion characteristics induced by gait variations, ultimately limiting model accuracy. In contrast, IMUNet employs DSC improving its ability to extract complex information and demonstrating robust performance in comparative experiments. Furthermore, none of the baseline models incorporate an attention mechanism to enhance the capture of long-term dependencies in sequences, a key factor in ResKACNNet. Consequently, the improvements achieved by ResKACNNet relative to these baselines are both justified and compelling.

Table II also presents re-training and inference results for

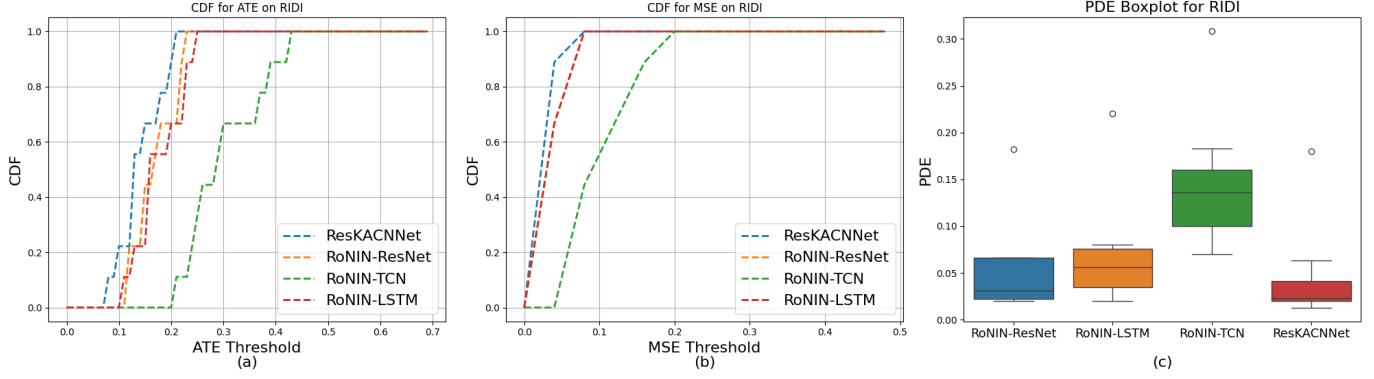


Fig. 3. Comparison of Cumulative Distribution Functions (CDFs) and Drift Error Performance (PDE) between ResKACNNNet and RoNIN Variant Models on the RIDI Dataset.

TABLE III
THE ABLATION STUDY RESULTS ON THE RoNIN, RIDI, IMUNET, RNIN-VIO, TLIO AND TLIOv2 DATASET.

| Dataset | Metric | RoNIN-ResNet | ResKACNNNet (wo EKSA) | ResKACNNNet |
|----------|--------|----------------------|-----------------------|--------------|
| | | Performance (meters) | | |
| RoNIN | ATE | 5.365 | 5.057 | 3.814 |
| | RTE | 3.390 | 3.215 | 3.272 |
| RIDI | ATE | 2.578 | 2.128 | 1.835 |
| | RTE | 2.823 | 2.198 | 1.954 |
| RNIN-VIO | ATE | 1.850 | 1.228 | 1.067 |
| | RTE | 2.185 | 1.346 | 1.260 |
| IMUNet | ATE | 14.207 | 9.578 | 9.023 |
| | RTE | 7.946 | 7.375 | 7.082 |
| TLIO | ATE | 1.476 | 1.430 | 1.420 |
| | RTE | 3.790 | 3.552 | 3.509 |
| TLIOv2 | ATE | 1.328 | 1.331 | 1.322 |
| | RTE | 1.105 | 1.117 | 1.118 |

each model on the gravity-compensated dataset TLIOv2. The experimental outcomes reveal that, with the exception of RoNIN-TCN, most models exhibit significant reductions in both ATE and RTE when evaluated on TLIOv2, compared to the original dataset. Further analysis indicates that gravity removal does not alter the ranking of model performance, reinforcing that gravity removal enhances inertial positioning accuracy without fundamentally altering model effectiveness. This improvement is attributable to the gravity component in the acceleration data, which causes the x and y axes to register values an order of magnitude lower than the z axis, thereby obscuring the true motion information.

Fig. 2 illustrates representative sample trajectories selected from the test sets of the various datasets to visually compare the performance of the ResKACNNNet and RoNIN-ResNet architectures. The selected sample trajectories represent a variety of real-world motion states: in the simple trajectories shown in Fig. 2(d) and Fig. 2(e), the predicted trajectory from RoNIN-ResNet gradually deviates from the true direction due to the accumulation of heading errors, while ResKACNNNet, which effectively models long-term dependencies and exhibits stronger noise resistance, more accurately recovers the trajectory. In Fig. 2(b), Fig. 2(c), Fig. 2(d), and Fig. 2(f), RoNIN-ResNet exhibits noticeable deviations after rotations

and other complex motions, while ResKACNNNet continues to effectively capture these complex nonlinear motion characteristics, achieving long and intricate trajectory positioning.

E. Ablation Study

In this section, we assess the overall performance of the ResKACNNNet model, as well as the effectiveness of its core modules, ResChebyKAN and EKSA.

1) *Model Performance Evaluation*: Fig. 3 presents the experimental results for ResKACNNNet and three RoNIN variants on the sampled dataset. Fig. 3(a) and Fig. 3(b) show the cumulative distribution functions (CDFs) for the entire dataset. Notably, the blue curve representing ResKACNNNet is steeper, indicating that it achieves significantly lower ATE and MSE errors compared to all RoNIN variants. Furthermore, Fig. 3(c) demonstrates that ResKACNNNet excels in minimizing drift error (PDE), which reflects its superior ability to converge more accurately to the final position. These results highlight that ResKACNNNet provides a more accurate and reliable positioning reference for inertial positioning tasks.

2) *Module Effectiveness*: To assess the efficacy of the proposed modules, we performed experiments comparing three model variants: RoNIN-ResNet, the complete ResKACNNNet, and a ResKACNNNet variant without the attention module, denoted as ResKACNNNet(wo EKSA). As shown in Table III, ResKACNNNet(wo EKSA) achieves lower error rates on both the ATE and RTE metrics compared to RoNIN-ResNet, demonstrating the effectiveness of the ResChebyKAN backbone. Moreover, the addition of the EKSA module further reduces errors, enhancing velocity prediction accuracy. These findings validate the significant contributions of both ResChebyKAN and EKSA to the overall performance of ResKACNNNet.

V. CONCLUSION

In this study, we propose ResKACNNNet, an inertial positioning network that integrates ResChebyKAN and EKSA to enhance nonlinear feature extraction and long-term dependency modeling. We also quantitatively analyze the impact of gravity on inertial positioning accuracy and provide preprocessed

datasets for future research. A key limitation of ResKACNNNet is the accumulation of heading errors due to the absence of explicit heading estimation and correction mechanisms. In future work, we plan to incorporate direction estimation strategies to mitigate drift errors and further improve positioning accuracy.

REFERENCES

- [1] A. K. Panja, C. Chowdhury, and S. Neogy, "Survey on inertial sensor-based ils for smartphone users," *CCF Transactions on Pervasive Computing and Interaction*, vol. 4, no. 3, pp. 319–337, 2022.
- [2] R. Harle, "A survey of indoor inertial positioning systems for pedestrians," *IEEE Communications Surveys & Tutorials*, vol. 15, no. 3, pp. 1281–1293, 2013.
- [3] P. G. Savage, "Strapdown inertial navigation integration algorithm design part 2: Velocity and position algorithms," *Journal of Guidance, Control, and Dynamics*, vol. 21, no. 2, pp. 208–221, 1998.
- [4] A. Nayak, A. Eskandarian, Z. Doerzaph, and P. Ghorai, "Pedestrian trajectory forecasting using deep ensembles under sensing uncertainty," *IEEE Transactions on Intelligent Transportation Systems*, vol. 25, no. 9, pp. 11 317–11 329, 2024.
- [5] R. P. Suresh, V. Sridhar, J. Pramod, and V. Talasila, "Zero velocity potential update (zupt) as a correction technique," in *Proceedings of the 2018 3rd International Conference On Internet of Things: Smart Innovation and Usages (IoT-SIU)*, 2018, pp. 1–8.
- [6] S. Herath, H. Yan, and Y. Furukawa, "Ronin: Robust neural inertial navigation in the wild: Benchmark, evaluations, & new methods," in *2020 IEEE International Conference on Robotics and Automation (ICRA)*, 2020, pp. 3146–3152.
- [7] K. He, X. Zhang, S. Ren, and J. Sun, "Deep residual learning for image recognition," in *Proceedings of the 2016 IEEE Conference on Computer Vision and Pattern Recognition (CVPR)*, 2016, pp. 770–778.
- [8] C. Lea, R. Vidal, A. Reiter, and G. D. Hager, "Temporal convolutional networks: A unified approach to action segmentation," in *Computer Vision – ECCV 2016 Workshops*, G. Hua and H. Jégou, Eds. Cham: Springer International Publishing, 2016, pp. 47–54.
- [9] S. Hochreiter and J. Schmidhuber, "Long short-term memory," *Neural Computation*, vol. 9, no. 8, pp. 1735–1780, 1997.
- [10] W. Liu, D. Caruso, E. Ilg, J. Dong, A. I. Mourikis, K. Daniilidis, V. Kumar, and J. Engel, "Tlio: Tight learned inertial odometry," *IEEE Robotics and Automation Letters*, vol. 5, no. 4, pp. 5653–5660, 2020.
- [11] A. I. Mourikis and S. I. Roumeliotis, "A multi-state constraint kalman filter for vision-aided inertial navigation," in *Proceedings of the 2007 IEEE International Conference on Robotics and Automation*, 2007, pp. 3565–3572.
- [12] D. Chen, N. Wang, R. Xu, W. Xie, H. Bao, and G. Zhang, "Rninvio: Robust neural inertial navigation aided visual-inertial odometry in challenging scenes," in *2021 IEEE International Symposium on Mixed and Augmented Reality (ISMAR)*, 2021, pp. 275–283.
- [13] R. Doorshi, H. Saleem, and R. Malekian, "Enhancing visual inertial odometry performance using deep learning-based sensor fusion," in *Proceedings of the 2024 IEEE International Conferences on Internet of Things (iThings), IEEE Green Computing & Communications (Green-Com), IEEE Cyber, Physical & Social Computing (CPSCom), IEEE Smart Data (SmartData), and IEEE Congress on Cybermatics*, 2024, pp. 112–117.
- [14] B. Zeinali, H. Zanddizari, and M. J. Chang, "Imunet: Efficient regression architecture for inertial imu navigation and positioning," *IEEE Transactions on Instrumentation and Measurement*, vol. 73, no. 2516213, 2024.
- [15] M. Sandler, A. Howard, M. Zhu, A. Zhmoginov, and L.-C. Chen, "Mobilenetv2: Inverted residuals and linear bottlenecks," in *Proceedings of the IEEE conference on computer vision and pattern recognition*, 2018, pp. 4510–4520.
- [16] A. G. Howard, M. Zhu, B. Chen, D. Kalenichenko, W. Wang, T. Weyand, M. Andreetto, and H. Adam, "Mobilenets: Efficient convolutional neural networks for mobile vision applications," 2017. [Online]. Available: <https://arxiv.org/abs/1704.04861>
- [17] M. Tan, B. Chen, R. Pang, V. Vasudevan, M. Sandler, A. Howard, and Q. V. Le, "Mnasnet: Platform-aware neural architecture search for mobile," in *Proceedings of the IEEE/CVF conference on computer vision and pattern recognition*, 2019, pp. 2820–2828.
- [18] M. Tan and Q. Le, "Efficientnet: Rethinking model scaling for convolutional neural networks," in *International conference on machine learning*. PMLR, 2019, pp. 6105–6114.
- [19] Y. Wang, H. Cheng, A. Zhang, and M. Q.-H. Meng, "From imu measurement sequence to velocity estimate sequence: An effective and efficient data-driven inertial odometry approach," *IEEE Sensors Journal*, vol. 23, no. 15, pp. 17 117–17 126, 2023.
- [20] A. Brajdic and R. Harle, "Walk detection and step counting on unconstrained smartphones," in *Proceedings of the 2013 ACM International Joint Conference on Pervasive and Ubiquitous Computing*, ser. UbiComp '13. New York, NY, USA: Association for Computing Machinery, 2013, p. 225–234. [Online]. Available: <https://doi.org/10.1145/2493432.2493449>
- [21] C. Chen, X. Lu, A. Markham, and N. Trigoni, "Ionet: Learning to cure the curse of drift in inertial odometry," in *Proceedings of the AAAI Conference on Artificial Intelligence*, vol. 32, no. 1, 2018.
- [22] H. Yan, Q. Shan, and Y. Furukawa, "Ridi: Robust imu double integration," in *Computer Vision – ECCV 2018*, V. Ferrari, M. Hebert, C. Sminchisescu, and Y. Weiss, Eds. Cham: Springer International Publishing, 2018, pp. 641–656.
- [23] M. Hearst, S. Dumais, E. Osuna, J. Platt, and B. Scholkopf, "Support vector machines," *IEEE Intelligent Systems and their Applications*, vol. 13, no. 4, pp. 18–28, 1998.
- [24] C. L. Gentil, F. Tschopp, I. Alzugaray, T. Vidal-Calleja, R. Siegwart, and J. Nieto, "Idol: A framework for imu-dvs odometry using lines," 2020, arXiv:2008.05749.
- [25] X. Cao, C. Zhou, D. Zeng, and Y. Wang, "Rio: Rotation-equivariance supervised learning of robust inertial odometry," in *2022 IEEE/CVF Conference on Computer Vision and Pattern Recognition (CVPR)*, 2022, pp. 6604–6613.
- [26] B. Rao, E. Kazemi, Y. Ding, D. M. Shila, F. M. Tucker, and L. Wang, "Ctin: Robust contextual transformer network for inertial navigation," *Proceedings of the AAAI Conference on Artificial Intelligence*, vol. 36, no. 5, pp. 5413–5421, Jun. 2022. [Online]. Available: <https://ojs.aaai.org/index.php/AAAI/article/view/20479>
- [27] S. M. Nguyen, L. D. Tran, D. Viet Le, and P. J. M. Havinga, "iMoT: Inertial Motion Transformer for Inertial Navigation," *arXiv e-prints*, p. arXiv:2412.12190, Dec. 2024.
- [28] Z. Liu, Y. Wang, S. Vaidya, F. Ruehle, J. Halverson, M. Soljačić, T. Y. Hou, and M. Tegmark, "Kan: Kolmogorov-arnold networks," 2024, arXiv:2404.19756.
- [29] X. Yang and X. Wang, "Kolmogorov-arnold transformer," in *The Thirteenth International Conference on Learning Representations*, 2025. [Online]. Available: <https://openreview.net/forum?id=BCeock53nt>
- [30] I. Drokina, "Kolmogorov-arnold convolutions: Design principles and empirical studies," 2024, arXiv:2407.01092.
- [31] SynodicMonth, "Cheykan," <https://github.com/SynodicMonth/CheyKAN.git>, 2024.
- [32] Z. Bozorgasl and H. Chen, "Wav-kan: Wavelet kolmogorov-arnold networks," 2024, arXiv:2405.12832.
- [33] A. Vaswani, N. Shazeer, N. Parmar, J. Uszkoreit, L. Jones, A. N. Gomez, L. Kaiser, and I. Polosukhin, "Attention is all you need," in *Proceedings of the 31st International Conference on Neural Information Processing Systems*, ser. NIPS'17. Red Hook, NY, USA: Curran Associates Inc., 2017, p. 6000–6010.
- [34] M. Zhang, C. Zhang, Q. Zhang, J. Guo, X. Gao, and J. Zhang, "Essaformer: Efficient transformer for hyperspectral image super-resolution," in *2023 IEEE/CVF International Conference on Computer Vision (ICCV)*, 2023, pp. 23 016–23 027.
- [35] J. Sturm, N. Engelhard, F. Endres, W. Burgard, and D. Cremers, "A benchmark for the evaluation of rgb-d slam systems," in *Proceedings of the 2012 IEEE/RSJ International Conference on Intelligent Robots and Systems*, 2012, pp. 573–580.